

Element-specific x-ray circular magnetic dichroism of Co_2MnGe Heusler thin films

J. Grabis,* A. Bergmann, A. Nefedov, K. Westerholt, and H. Zabel

Ruhr-Universität Bochum, 44780 Bochum, Germany

(Received 30 August 2004; revised manuscript received 4 November 2004; published 19 July 2005)

We report measurements of x-ray absorption spectra and x-ray magnetic circular dichroism (XMCD) on thin films of the ferromagnetic Heusler compound Co_2MnGe at the $L_{2,3}$ edges of Mn and Co. While the Co spectra are similar to those of metallic Co, the Mn spectra indicate partly localized $3d$ electrons, which we attribute to Mn atoms at the interface with the Au protection layer. We have analyzed the XMCD spectra using sum rules in order to estimate the element-specific magnetic moments. We find that the decrease of the thin film magnetization as compared to the bulk is mainly caused by a reduction of the Mn moments.

DOI: [10.1103/PhysRevB.72.024437](https://doi.org/10.1103/PhysRevB.72.024437)

PACS number(s): 81.15.Cd, 75.70.-i, 85.75.-d, 78.70.Dm

I. INTRODUCTION

According to band structure calculations several Heusler compounds, such as PtMnSb , NiMnSb ,¹ Co_2MnSi , Co_2MnGe ,² and $\text{Co}_2\text{Cr}_{0.6}\text{Fe}_{0.4}\text{Al}$ (Ref. 3) are half-metallic ferromagnets, i.e., they possess a gap in the minority-spin band at the Fermi level and therefore a spin polarization of 100%.⁴ This property makes these Heusler compounds attractive candidates for applications in giant magnetoresistance (GMR) and tunneling magnetoresistance (TMR) devices and as electrodes for spin-polarized current injection into semiconductors.

The Heusler alloy Co_2MnGe under study here grows in the $L2_1$ structure—a cubic lattice combining four fcc sublattices occupied by the Co, Mn, and Ge atoms, respectively. Since the narrow gap in the minority-spin band at the Fermi energy is induced by symmetry,⁴ any deviation from perfect site order in the Heusler unit cell can severely affect the degree of spin polarization of the system.^{5,6} Perfectly ordered $L2_1$ symmetry is difficult to achieve even in bulk single crystals of the Heusler phase. In thin film heterostructures, which must be processed at rather low temperatures in order to prevent excessive interdiffusion at the interface, site disorder can hardly be avoided completely. Thus the presence of site disorder has been suggested to be the main reason for the moderate performance of GMR and TMR devices based on the fully spin-polarized Heusler compounds achieved until now.^{7,8}

Recent theoretical model calculations of the electronic and magnetic properties of typical point defects in the Co_2MnSi and Co_2MnGe phases have elucidated this point essentially.⁹ A Mn antisite defect, i.e., a Mn atom at a regular Co position in the ordered $L2_1$ lattice, has its magnetic moment antiparallel to the nearest-neighbor Mn and Co moments, due to the antiferromagnetic exchange coupling between nearest-neighbor Mn atoms. Since in this case the Mn moment counts twice, this type of defect will drastically reduce the ferromagnetic magnetization. Co antisite defects, on the other hand, retain their ferromagnetic spin orientation and the magnetic moment remains virtually unchanged.⁹ However, these defects contribute electronic states in the minority-spin gap, i.e., very effectively destroy the half metallicity of the films. These calculations offer a reasonable explanation for the reduced ferromagnetic saturation magne-

tization observed in thin films of the Co_2MnGe phase when prepared at low temperatures.¹⁰

An ideal tool to study the element-specific magnetic moments directly is x-ray magnetic circular dichroism (XMCD). We report an experimental investigation of XMCD spectra of a thin Co_2MnGe film here. A previous XMCD measurement on the Co_2MnGe phase published in the literature deals, with a bulk sample with a saturation magnetization close to the theoretical value for ideal $L2_1$ order.¹¹

II. PREPARATION AND EXPERIMENT

A thin film with a nominal thickness of 11 nm of the Co_2MnGe phase was prepared on a sapphire a -plane substrate, as described in detail elsewhere.^{10,12} To induce a high-quality (110) textured growth a vanadium seed layer with a thickness of 2 nm was sputtered before the deposition of the Co_2MnGe film. The film was covered by a 2 nm gold cap layer. Au is known to wet the Co_2MnGe surface,¹⁰ and this thickness is sufficient to provide a perfect protection against oxidation of the surface. This is essential for the analysis below, since x-ray absorption spectroscopy (XAS) measured in total electron yield mode (TEY) probes a surface layer of a few nanometers total thickness due to the electron escape depth, i.e., the method is rather surface sensitive.¹³

The Co_2MnGe film of the present study was prepared at a substrate temperature of 300 °C. Whereas at a growth temperature of 500 °C Co_2MnGe films develop about 95% of the theoretical saturation magnetization (corresponding to $5\mu_B$ per formula unit), at 300 °C there is a strong reduction of the saturation magnetization to about 60% of the theoretical value.¹² Since our main interest was to investigate the microscopic origin of this moment reduction, we used a film prepared at 300 °C for the XMCD study. Our film had a saturation magnetization of $(2.98 \pm 0.1)\mu_B$ per formula unit at 5 K as measured by superconducting quantum interference device (SQUID) magnetometry. At room temperature, where the XAS and the XMCD spectra were taken, the saturation magnetization was $2.32\mu_B$ per formula unit.

The structural quality of the film was characterized by hard x-ray scattering using a Cu $K\alpha$ rotating-anode x-ray tube. A low-angle hard x-ray reflectivity scan is shown in

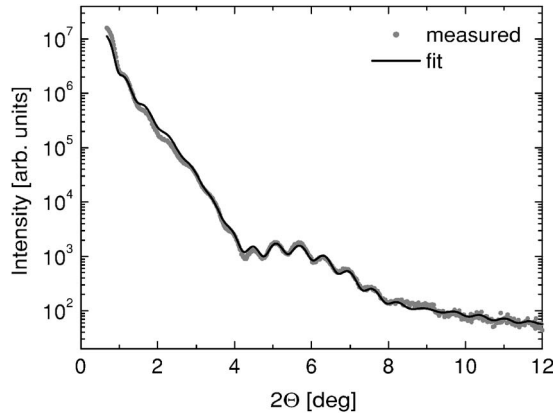


FIG. 1. X-ray reflectivity measured with a standard Cu $K\alpha$ rotating-anode x-ray tube. From a fit to the experimental data the layer thicknesses are 11.1 nm for Co_2MnGe and 2.13 nm for Au. The roughnesses are 0.33 and 0.18 nm for Co_2MnGe and Au.

Fig. 1. Film thickness oscillations observed up to $2\Theta=10^\circ$ reveal the smooth surfaces and interfaces of the film. A fit of the reflectivity by the Parratt formalism¹⁴ gives roughness parameters of $\sigma=0.18$ and 0.33 nm for the Au and the Co_2MnGe layer, respectively. Atomic force microscopy pictures of the sample surface reveal an atomically flat film with a rms roughness of 0.1–0.2 nm. In large-angle x-ray diffraction only the (220) and (440) Bragg reflections occur, proving that the sample has grown with pure (110) texture out of plane. XAS and XMCD were measured at the bending magnet beamline PM3 at BESSY II (Berlin, Germany) using the ALICE diffractometer.¹⁵ The energy resolution was set to approximately $\Delta E/E=1\times 10^{-4}$. All absorption spectra were taken by the TEY method, i.e., by measuring the sample drain current. XMCD spectra were measured with fixed helicity and alternating magnetic field $B=\pm 0.11$ T parallel to the sample surface. The degree of circular polarization P_c was approx. 95%. The angle of incidence was chosen to be 40° with respect to the surface. At this angle saturation effects are supposed to be small.^{13,16} The TEY signal is therefore assumed to be proportional to the absorption coefficient, $Y_\pm \sim \hbar\omega\mu_\pm(\hbar\omega)$, where \pm denotes the magnetic field direction parallel (+) or antiparallel (–) to the photon helicity. The Y_+ and Y_- spectra have been corrected for a small offset (<1%) in the pre- L_3 - and post- L_2 -edge regions, due to different electron trajectories in the external magnetic field.¹⁷ The spectra were normalized to the incoming photon flux. All measurements have been performed at room temperature.

III. RESULTS AND DISCUSSION

The averaged x-ray absorption spectra $(Y_+ + Y_-)/2$ at the Mn and Co $L_{2,3}$ edges are shown in Fig. 2. The Mn spectrum shows a multiplet structure at the L_3 edge with peaks at 1.5 and 3.5 eV above the absorption edge maximum and a doublet structure at the L_2 absorption edge. These features have not been observed in bulk Co_2MnGe Heusler samples with surfaces prepared *in situ*.¹¹ The multiplet structure is a clear

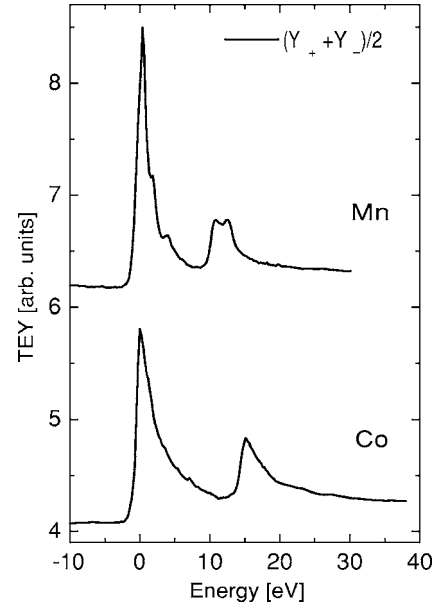


FIG. 2. XAS spectra at the Mn and Co $L_{2,3}$ edges. The photon energy is defined with respect to the L_3 peak position.

sign of localized $3d$ electrons. Calculated absorption spectra of Mn in the ${}^6S_{5/2}$ ground state, the atomic high-spin ground state of Mn, show the same multiplet structure.^{11,18,19} The transition from the localized high-spin ground state to the itinerant low-spin ground state of metallic Mn has been described by Dürr *et al.*²⁰ A strong localization of Mn $3d$ electrons has been observed mainly in two systems: Mn atoms in a noble metal environment with completely filled $3d$ shells^{18,21} and oxidized Mn.^{22,23} We think the first interpretation holds in our case, since the film is protected by a Au cap layer preventing oxidation. Therefore we attribute the multiplet structure to Mn atoms at the interface with the Au cap layer.

The Co XAS shown in Fig. 2 is much broader. The shape is very similar to that of pure metallic Co; multiplet structures as typical for CoO are not present.²⁴ A small shoulder-like structure is seen 1 eV above the L_3 absorption maximum. A more pronounced structure at the same energy has been observed by Miyamoto *et al.* and has been interpreted as an optical transition to the unoccupied minority t_{2g} states in the Co partial density of states.^{4,11}

The localized (itinerant) character of the Mn (Co) $3d$ states can be further quantified by the branching ratio $R = A(2p_{3/2})/[A(2p_{1/2}) + A(2p_{3/2})]$, which is the ratio of background-corrected integrated intensities at the corresponding absorption edges.^{20,25} For this purpose the XAS data have been adjusted to tabulated absorption coefficients²⁶ in the pre- L_3 and post- L_2 energy regions for Mn and Co, respectively. To subtract the steplike increase of intensity, an arctan function has been used.³ The function mimics a step of 2/3 and 1/3 of the total step height at the L_3 and L_2 edge energy, respectively, corresponding to the number of electrons in the core state. The steps are broadened over an energy range $\Delta E=0.2$ eV due to finite instrumental resolution, temperature, and final-state lifetime. For Mn one finds a branching ratio of $R=0.74$, close to the value for atomic Mn.

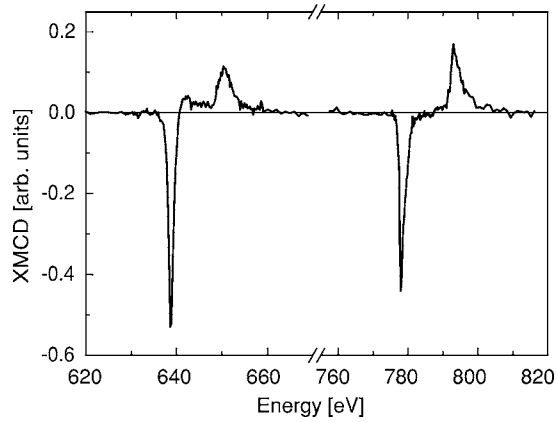


FIG. 3. XMCD spectra at the Mn and Co $L_{2,3}$ edges.

The Co branching ratio is $R=0.68$. Within the error bars of the measurement this corresponds to the statistical value of $2/3$ expected for a metal with neither core-valence electron correlation nor spin-orbit splitting of the conduction band.

XMCD spectra $Y_+ - Y_-$ at the Mn and Co $2p \rightarrow 3d$ absorption edges are displayed in Fig. 3. The difference signal has been corrected for the degree of circular polarization and the angle of incidence. Within the noise level of the experiment no multiplet structure can be resolved either at the Mn or at the Co absorption edge. This is interesting in comparison to the XAS spectrum of Mn in Fig. 3 where a multiplet structure is clearly observed, suggesting that the XAS spectrum results from a superposition of a nonferromagnetic layer at the interface and a ferromagnetic bulk layer. The XMCD spectrum only probes the ferromagnetic bulk layer which does not exhibit a multiplet structure.

We analyzed the XMCD measurements quantitatively by performing a sum rule analysis in order to determine the element-specific orbital and spin magnetic moments.^{27,28} This procedure might evoke large systematic errors for several reasons. First, the number of $3d$ holes n_h is inaccessible experimentally and has to be taken from band structure calculations, yielding $n_h=2.196$ and $n_h=4.488$ for Co and Mn, respectively.⁴ Second, the spin magnetic dipole term $\langle T_z \rangle$ is assumed to be negligible. Principally this assumption seems justified for Co_2MnGe because of the cubic symmetry of the system. However, due to the symmetry breaking at the interface the magnetic dipole term could be of importance here. Furthermore, in the case of Mn the spin sum rule analysis is problematic because $2p$ - $3d$ electrostatic interactions are large compared to $2p$ spin-orbit coupling, leading to an overlap of L_3 and L_2 edges and a mixing between the two j levels. Dürr *et al.* gave a correction factor $\xi=1.5$ for jj mixing in Mn.^{20,23} Keeping these systematic errors in mind, the sum rule analysis of the Co XMCD spectrum yields $m_{\text{spin}}=0.55\mu_B$ per atom and $m_{\text{orb}}=0.028\mu_B$ per atom. The Mn moments are $m_{\text{spin}}=(0.98-1.47)\mu_B$ per atom, depending on the value assumed for ξ , and $m_{\text{orb}}=0.056\mu_B$ per atom.

The magnetic moments obtained from the XMCD spectra can be compared to the integral magnetic moment measured by SQUID-based magnetometry. SQUID measurements at room temperature yield a magnetic moment of $m=2.32\mu_B$ per formula unit. The total magnetic moment at 5 K is

TABLE I. Element-specific atomic magnetic moments m determined by XMCD, magnetometry, and band structure calculations (Ref. 4). For a better comparison of XMCD experiments and theory, the element-specific moments measured at room temperature (RT) have been extrapolated to 5 K. The range of values given for the Mn magnetic moment corresponds to the upper and lower limits of the jj mixing correction factor.

$m(\mu_B)$	Theory	RT	5 K
Mn	3.61	1.04–1.53 (XMCD)	1.36–1.97 (XMCD)
Co	0.75	0.58 (XMCD)	0.75 (XMCD)
Co_2MnGe	5	2.2–2.69 (XMCD)	2.83–3.46 (XMCD)
Co_2MnGe		2.32(12) (SQUID)	2.98(15) (SQUID)

$2.98\mu_B$ per formula unit. Correcting the atomic magnetic moments determined by XMCD at room temperature by the same factor we get the magnetic saturation moments of Co and Mn given in the last column of Table I, which can be compared directly to the theoretical moments.

Both the magnetic moments of Co and Mn are found to be reduced compared to the theoretical moment for a fully ordered Heusler compound. However, the Mn magnetic moments seem to be more significantly affected. The Co moment is about 20% lower than the theoretical value; the Mn moment is reduced by 30% to more than 50%, depending on the model assumption. The electronic band structure calculations show that the Co atomic moment is hardly changed by antisite disorder whereas antisite Mn atoms have a spin direction antiparallel to the neighboring Mn moments and contribute a moment of $-1.4\mu_B$ compared to $3.04\mu_B$ on a regular Mn position. The observation of the reduced Co moment again points toward the existence of a nonferromagnetic interface layer between the Co_2MnGe layer and the Au cap layer. Assuming that the rms roughness of 0.33 nm can be identified with the interface thickness and taking into consideration the enhanced weight of the surface atoms in the total electron yield method, the observed Co moment reduction seems plausible. The additional stronger loss of the Mn atomic magnetic moments should be attributed to the site disorder in the bulk of the film which, as stated above, gives rise to a strong reduction of the Mn sublattice magnetization whereas the Co magnetization is hardly affected.

IV. SUMMARY AND CONCLUSION

The analysis of the element-specific soft x-ray absorption and magnetic circular dichroism on the Co and Mn $L_{2,3}$ edges of a Co_2MnGe thin film revealed a rather different behavior of the Co and Mn atoms. The XAS of Mn presents a pronounced multiplet structure which we attribute to Mn atoms with partly localized wave functions at the Au interface. The sum rule analysis of the XMCD spectra yields atomic magnetic moments for Mn and Co definitely lower than the theoretical values but consistent with bulk magnetization measurements. We have tentatively attributed the smaller atomic magnetic moments to the existence of a nonferromagnetic interlayer close to the Au cap layer. This hy-

pothesis, which was originally motivated by the bulk magnetic properties on $[\text{Co}_2\text{MnGe}/\text{Au}]_n$ multilayers,²⁹ recently found strong support in the analysis of x-ray resonant magnetic reflectivity (XRMR) measurements on the $[\text{Co}_2\text{MnGe}/\text{Au}]_n$ multilayers.³⁰ From the XRMR data one can reliably derive a magnetization profile along the growth direction of the multilayer. This revealed the existence of a nonferromagnetic layer of about 0.3 nm thickness at the $\text{Co}_2\text{MnGe}/\text{Au}$ interface at room temperature. An additional atomic magnetic moment reduction is caused by antisite disorder in the bulk of the thin film, which mainly affects the Mn spins.

The high degree of site disorder in the film that is suggested by the strongly reduced Mn magnetic moments is qualitatively consistent with magnetotransport data¹² revealing the small electronic mean free path of the order of 2 nm at 4 K and a strong isotropic spin disorder magnetoresis-

tance. The half metallicity of the ideal Co_2MnGe compound cannot be expected for the film under study here, because the electronic states of point defects will fill the gap in the density of states of the minority-spin band. The results presented here point out the difficulties one will encounter when trying to use the full spin polarization of the Heusler compounds in TMR and GMR devices. Without high-temperature processing providing a high degree of metallurgical order of the Heusler phase, the performance will not be superior to that of conventional ferromagnetic transition metals.

ACKNOWLEDGMENTS

We would like to thank S. Erdt-Böhm for sample preparation and T. Kachel for his help with beamline operation. This project is funded by BMBF Grants No. 03ZA6BC2 and No. 05ES3XBA/5 and SFB 491.

*Electronic address: johannes.grabis@ruhr-uni-bochum.de

- ¹R. A. de Groot, F. M. Mueller, P. G. van Engen, and K. H. J. Buschow, *Phys. Rev. Lett.* **50**, 2024 (1983).
- ²S. Ishida, T. Masaki, S. Fujii, and S. Asano, *Physica B* **245**, 1 (1998).
- ³H. J. Elmers *et al.*, *Phys. Rev. B* **67**, 104412 (2003).
- ⁴I. Galanakis, P. H. Dederichs, and N. Papanikolaou, *Phys. Rev. B* **66**, 174429 (2002).
- ⁵D. Orgassa, H. Fujiwara, T. C. Schulthess, and W. H. Butler, *Phys. Rev. B* **60**, 13237 (1999).
- ⁶W. R. Branford *et al.*, *Phys. Rev. B* **69**, 201305(R) (2004).
- ⁷M. C. Kautzky, F. B. Mancoff, J.-F. Bobo, P. R. Johnson, R. L. White, and B. M. Clemens, *J. Appl. Phys.* **81**, 4026 (1997).
- ⁸M. P. Raphael, B. Ravel, M. A. Willard, S. F. Cheng, B. N. Das, R. M. Stroud, K. M. Bussmann, J. H. Claassen, and V. G. Harris, *Appl. Phys. Lett.* **79**, 4396 (2001).
- ⁹S. Picozzi, A. Continenza, and A. J. Freeman, *Phys. Rev. B* **69**, 094423 (2004).
- ¹⁰U. Geiersbach, A. Bergmann, and K. Westerholt, *Thin Solid Films* **425**, 226 (2003).
- ¹¹K. Miyamoto, K. Iori, A. Kimura, T. Xie, M. Taniguchi, S. Qiao, and K. Tsuchiya, *Solid State Commun.* **128**, 163 (2003).
- ¹²U. Geiersbach, A. Bergmann, and K. Westerholt, *J. Magn. Magn. Mater.* **240**, 546 (2002).
- ¹³W. L. O'Brien and B. P. Tonner, *Phys. Rev. B* **50**, 12672 (1994).
- ¹⁴L. G. Parratt, *Phys. Rev.* **95**, 359 (1954).
- ¹⁵J. Grabis, A. Nefedov, and H. Zabel, *Rev. Sci. Instrum.* **74**, 4048 (2003).

- ¹⁶V. Chakarian, Y. U. Idzerda, and C. T. Chen, *Phys. Rev. B* **57**, 5312 (1998).
- ¹⁷E. Goering, A. Fuss, W. Weber, J. Will, and G. Schütz, *J. Appl. Phys.* **88**, 5920 (2000).
- ¹⁸B. T. Thole, R. D. Cowan, G. A. Sawatzky, J. Fink, and J. C. Fuggle, *Phys. Rev. B* **31**, 6856 (1985).
- ¹⁹W. L. O'Brien and B. P. Tonner, *Phys. Rev. B* **51**, 617 (1995).
- ²⁰H. A. Dürr, G. van der Laan, D. Spanke, F. U. Hillebrecht, and N. B. Brookes, *Phys. Rev. B* **56**, 8156 (1997).
- ²¹U. Arp, F. Federmann, E. Källne, B. Sonntag, and S. L. Sorensen, *J. Phys. B* **25**, 3747 (1992).
- ²²W. L. O'Brien and B. P. Tonner, *Phys. Rev. B* **58**, 3191 (1995).
- ²³Y. Yonamoto, T. Yokoyama, K. Amemiya, D. Matsumura, and T. Ohta, *Phys. Rev. B* **63**, 214406 (2001).
- ²⁴T. J. Regan, H. Ohldag, C. Stamm, F. Nolting, J. Lüning, J. Stöhr, and R. L. White, *Phys. Rev. B* **64**, 214422 (2001).
- ²⁵B. T. Thole and G. van der Laan, *Phys. Rev. B* **38**, 3158 (1988).
- ²⁶B. L. Henke, E. M. Gullikson, and J. C. Davis, *At. Data Nucl. Data Tables* **54**, 180 (1993).
- ²⁷B. T. Thole, P. Carra, F. Sette, and G. van der Laan, *Phys. Rev. Lett.* **68**, 1943 (1992).
- ²⁸P. Carra, B. T. Thole, M. Altarelli, and X. Wang, *Phys. Rev. Lett.* **70**, 694 (1993).
- ²⁹K. Westerholt, U. Geiersbach, and A. Bergmann, *J. Magn. Magn. Mater.* **257**, 239 (2003).
- ³⁰J. Grabis, A. Bergmann, A. Nefedov, K. Westerholt, and H. Zabel, following paper, *Phys. Rev. B* **72**, 024438 (2005).